ANALYSIS OF NON-NEWTONIAN FLOWS THROUGH CONTRACTIONS AND EXPANSIONS

Luiz A. Reis Junior
Department of Mechanical Engineering
Pontifícia Universidade Católica–Rio de Janeiro, RJ 22453-900, Brazil
lareis@hotmail.com

Mônica F. Naccache
Department of Mechanical Engineering
Pontifícia Universidade Católica–Rio de Janeiro, RJ 22453-900, Brazil
naccache@mec.puc-rio.br

Abstract. *Flow of non-Newtonian fluids through contractions and expansions are found in several industrial processes. In this work, a numerical simulation of non-Newtonian fluid flows through an axysimetric expansion followed by a contraction is performed. The numerical solution of conservation equations of mass and momentum is obtained via finite volume method. In order to model the non-Newtonian behavior of the fluid, it is used the Generalized Newtonian Fluid constitutive equation, with the Carreau viscosity function. The results obtained show the influence of rheological parameters on flow patterns.*

keywords: *Non-Newtonian fluids, contraction, expansion*

1. Introduction

In this work, the flow of non-Newtonian fluids through an abrupt axisymmetric expansion followed by an abrupt contraction is analyzed numerically. The mechanical behavior of the non-Newtonian fluid is modeled by the Generalized Newtonian Liquid constitutive equation (GNL) (Bird *et al.*, 1987):

$$\boldsymbol{\tau} = \eta(\dot{\gamma})\dot{\boldsymbol{\gamma}} \tag{1}$$

where $\boldsymbol{\tau}$ is the extra-stress tensor, $\dot{\boldsymbol{\gamma}}$ is the rate-of-deformation tensor, defined as $\mathrm{grad}\,\mathbf{v} + (\mathrm{grad}\,\mathbf{v})^{\mathrm{T}}$, $\mathbf{v}$ is the velocity vector and η is the viscosity function, given by the Carreau-Yasuda model:

$$\frac{\eta - \eta_\infty}{\eta_0 - \eta_\infty} = [1 + (\lambda\dot{\gamma})^a]^{(n-1)/a} \tag{2}$$

In this equation, η_0 is the viscosity at low shear rates, η_∞ is the viscosity at high shear rates, λ is a time constant, n is the power-law exponent, and a is a dimensionless parameter that describes the transition region between the zero-shear-rate region and the power-law region. Depending on the values of these parameters, this equation can be used to model viscoplastic materials. Viscoplastic materials are used in many industrial processes, and their main characteristic is the presence of a yield stress. Above the yield stress the material behaves as a liquid, and, below it, as a solid.

Barnes (1999a, 1999b) performed a comprehensive review about yield stress materials, reviving the argument that yield stress actually does not exist. He shows, for a large number of materials typically classified as viscoplastics, that when careful measurements are performed below the "yield stress," it is found that flow actually takes place. Then, the viscosity function looks like a bi-viscosity model, with very high viscosity at small shear rates and lower viscosities for larger shear rates. However, an apparent yield stress can exist as a useful mathematical description of limited data, over a given range of flow conditions.

Alexandrou *et al.* (2001) studied numerically the flow of Herschel-Bulkley fluids in a canonical three-dimensional expansion. The results were obtained for a 2:1 and a 4:1 expansion rate. The effects of Reynolds number and Bingham number on flow pattern and pressure distribution were investigated. It was observed that a strong interplay between the Reynolds and Bingham numbers occurs, and they influence the formation and break up of stagnant zones in the corner of the expansion. Souza Mendes *et al.* (2000) performed an experimental and numerical analysis of the flow of viscoplastic fluids through a converging-diverging channel. They observed experimentally a flow pattern transition, for a critical value of the ratio between the length and the diameter of the central region, indicating a possible material fracture. However, the viscosity model used in the numerical simulation was not capable to predict this behavior. The flow of Bingham materials through a 1×2 abrupt expansion was analyzed numerically by Vradis and Ötügen (1997). They observed that the reattachment length increases with Reynolds number and decreases with yield stress. Naccache and Souza Mendes (1997) studied numerically the flow of Bingham materials through abrupt expansions as a function of Reynolds number, yield stress and expansion ratio. It was noted that the reattachment length increases with the Reynolds number, decreases with yield stress and is essentially independent of the expansion ratio. An experimental study of the flow through axisymmetric
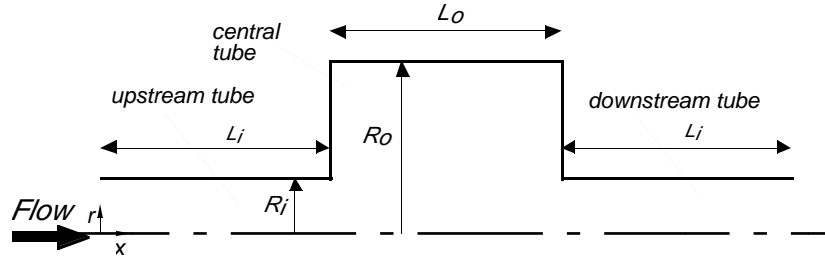
Figure 1: The geometry.

expansions was performed by Pak *et al.* (1990). This work analyzes the influence of Reynolds number on separation zones and reattachment length of Newtonian, purely viscous non-Newtonian, and viscoelastic fluids in abrupt axisymmetric expansions. It was observed that the reattachment length for purely viscous non-Newtonian fluids is almost the same as for Newtonian fluids. For laminar flows, elasticity decreases the reattachment length, while for turbulent flows the opposite trend is observed.

2. Analysis

The geometry analyzed is shown in Fig. 1. The flow is laminar, steady and axisymmetric. All the properties are considered to be constant and viscous dissipation is negligible.

The mass and momentum conservation equations for an incompressible fluid, and using the Generalized Newtonian Fluid constitutive equation, are given by:

$$\text{div}\mathbf{v} = 0 \tag{3}$$

$$\rho \text{grad}\mathbf{v} \cdot \mathbf{v} = -\text{grad}p + \text{div}(\eta \text{grad}\mathbf{v}) \tag{4}$$

where $\mathbf{v} = u\mathbf{i} + v\mathbf{j}$ is the velocity vector, u is the axial velocity component, v is the radial velocity component, p is the pressure, ρ is the fluid density, and η is the viscosity function, given by the Carreau model (eq. (2), with $a = 2$). Using cilindrical coordinates, the governing equations are given bellow.

Mass conservation equation:

$$\frac{1}{r}\frac{\partial}{\partial r}(rv) + \frac{\partial}{\partial x}(u) = 0 \tag{5}$$

Axial momentum conservation equation:

$$\frac{1}{r}\frac{\partial}{\partial r}(\rho rvu) + \frac{\partial}{\partial x}(\rho uu) = \frac{1}{r}\frac{\partial}{\partial r}\left(\eta r\frac{\partial u}{\partial r}\right) + \frac{\partial}{\partial x}\left(\eta\frac{\partial u}{\partial x}\right)$$

$$+\frac{1}{r}\frac{\partial}{\partial r}\left(\eta r\frac{\partial v}{\partial x}\right) + \frac{\partial}{\partial x}\left(\eta\frac{\partial u}{\partial x}\right) - \frac{\partial p}{\partial x} \tag{6}$$

Radial momentum conservation equation:

$$\frac{1}{r}\frac{\partial}{\partial r}(\rho rvv) + \frac{\partial}{\partial x}(\rho vu) = \frac{1}{r}\frac{\partial}{\partial r}\left(\eta r\frac{\partial v}{\partial r}\right) + \frac{\partial}{\partial x}\left(\eta\frac{\partial v}{\partial x}\right)$$

$$+\frac{1}{r}\frac{\partial}{\partial r}\left(\eta r\frac{\partial v}{\partial r}\right) + \frac{\partial}{\partial x}\left(\eta\frac{\partial u}{\partial r}\right) - 2\eta\frac{v}{r^2} - \frac{\partial p}{\partial r} \tag{7}$$

where x and r are the axial and radial coordinates, respectively.

The boundary conditions are the usual no-slip and impermeability conditions at solid boundaries ($u = v = 0$), the symmetry condition at centerline ($\partial u/\partial r = 0$ and $v = 0$), and developed flow at outlet ($\partial/\partial x = 0$). At the inlet, the axial velocity is considered uniform ($u = u_{mean}$ and $v = 0$). The length of upstream and downstream tubes was chosen to guarantee the flow development at the entrance of the central tube, and at the exit of the downstream tube ($L_i = 20R_i$).
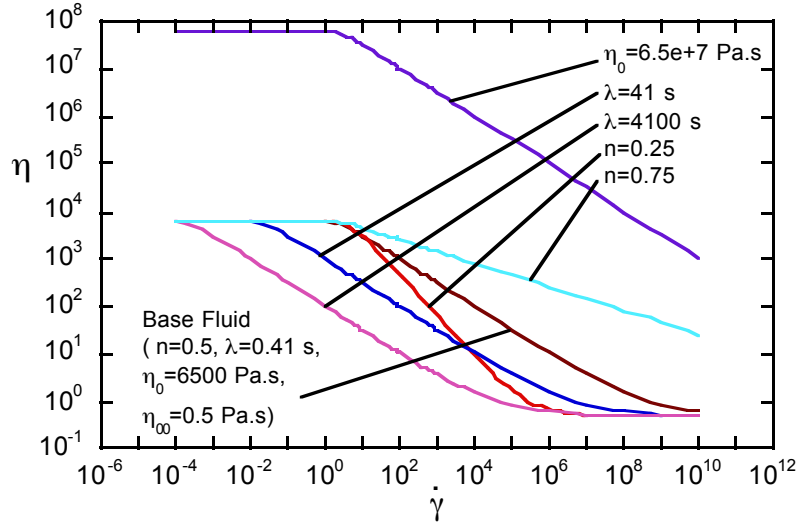
Figure 2: Viscosity function for the fluids analyzed.

3. Numerical Solution

The conservation equations of mass and momentum are discretized by the finite volume method described by Patankar (1980). Staggered velocity components are employed to avoid unrealistic pressure fields. The SIMPLE algorithm (Patankar, 1980) is used, in order to couple the pressure and velocity. The resulting algebraic system is solved by the TDMA line-by-line algorithm (Patankar, 1980) with the block correction algorithm (Settari and Aziz, 1973) to increase the convergence rate.

The mesh employed is uniform per zones in the axial and radial directions. To validate the numerical solution, extensive grid tests were performed. The error obtained for the product of the friction factor and the Reynolds number ($fRe = 8\dot{\gamma}_c D/\bar{u}$) with respect to the exact value, for a fully developed Newtonian flow at the downstream tube, was equal to 5%. For the non-Newtonian fluids, a comparison of deformation rates and velocity profiles obtained with the mesh used and finner meshes was performed, and similar results were obtained (Reis, 2003). Therefore, it was used a mesh with 300x120 control volumes in the axial and radial directions, respectively.

4. Results and discussions

All the numerical results obtained pertain to low Reynolds numbers ($Re = \rho\bar{v}D_o/\eta_c < 10^{-4}$), where η_c is the viscosity at the upstream tube wall. The influence of rheological parameters on flow patterns are analyzed for a fixed geometry: $R_o/R_i = 10$ and $L_o/R_o = 1$. Figure 2 shows the viscosity function for all the cases analyzed. The base fluid has the rheological properties of a Carbopol 676 water solution, given by: $\eta_0 = 6.5 \times 10^3$ Pa.s, $\eta_\infty = 0.5$ Pa.s, $\lambda = 0.41$ s^{-1}, $n = 0.5$, and $a = 2$. In this figure, it can be observed that the viscosity level increases with the parameter η_0, and the shear thinning behavior is delayed when time constant λ decreases. It can be also noted that as the power-law index n tends to unity, the shear thinning behavior becomes smoother.

Figure 3 shows the streamlines for the flow of the base fluid. It can be observed that a small recirculating zone appears near the corners. The viscosity function for this fluid is presented in Fig. 4. Higher levels of viscosity correspond to lower deformation rates. It can be noted that near the core region of the central tube, the deformation rates increase due to shear components, and the viscosity decreases. At the entrance and exit of the central tube, the deformation rates are larger due to extension, and the viscosity is also lower than near the wall region. It can also be observed that there is a zone near the wall of the central tube (radius R_o) where the viscosity reaches its largest value (i.e., $\eta = \eta_0$). In this region, the deformation rates are very low, and the flow is almost stagnant. This behavior could be interpreted as a material fracture, since the velocities at the core region are much higher than the ones observed near the walls (it's important to note that the viscosity model used can not predict a real stagnant flow). This result is similar to the ones obtained numerically and experimentally by Souza Mendes et $al.$ (2000), where a material fracture is observed experimentally near the core region of the central tube.

The effect of the power-law exponent on flow pattern can be analyzed with the aid of Figs. 5–8. These figures show the streamlines and viscosity function for $n = 0.25$ and $n = 0.75$. All other rheological parameters are held fixed.
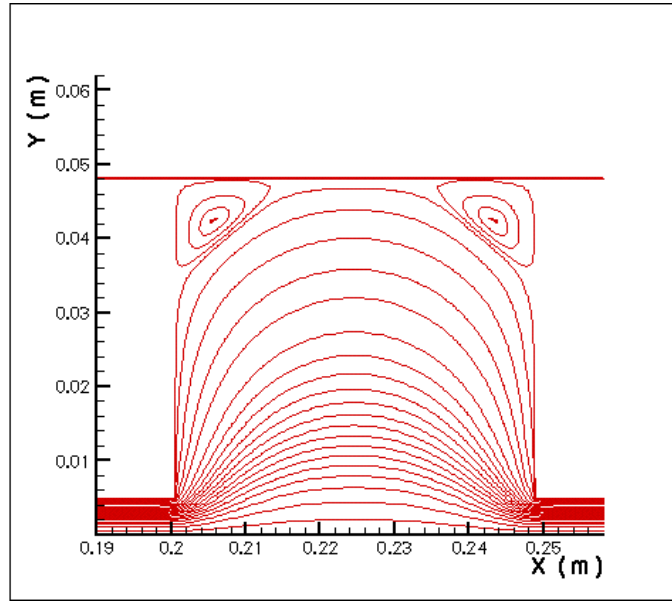
Figure 3: Streamlines. Base Fluid ($\eta_0 = 6.5 \times 10^3$ Pa.s, $\eta_\infty = 0.5$ Pa.s, $\lambda = 0.41$ s^{-1}, $n = 0.5$, and $a = 2$).

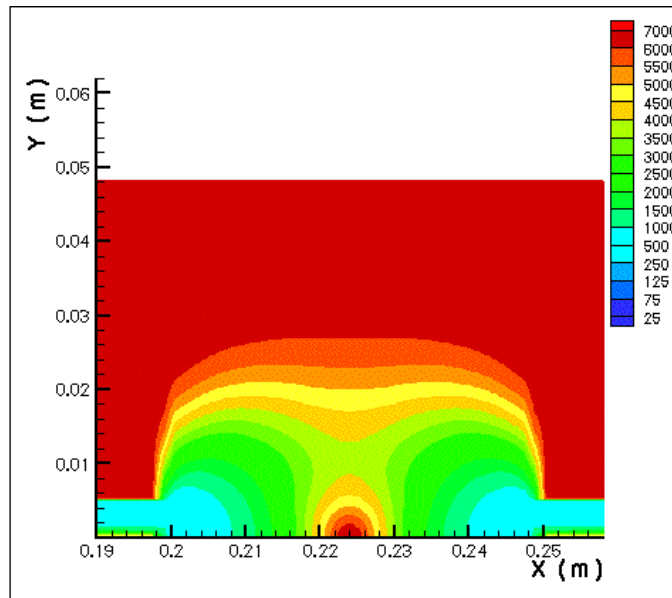Figure 4: Viscosity function. Base Fluid ($\eta_0 = 6.5 \times 10^3$ Pa.s, $\eta_\infty = 0.5$ Pa.s, $\lambda = 0.41$ s^{-1}, $n = 0.5$, and $a = 2$).
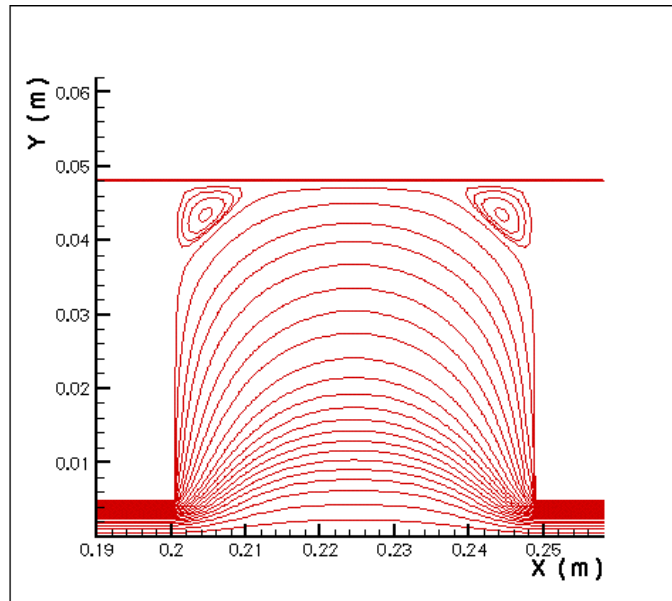
Figure 5: Streamlines, $\eta_0 = 6.5 \times 10^3$ Pa.s, $\eta_\infty = 0.5$ Pa.s, $\lambda = 0.41$ s^{-1}, $n = 0.25$, and $a = 2$.
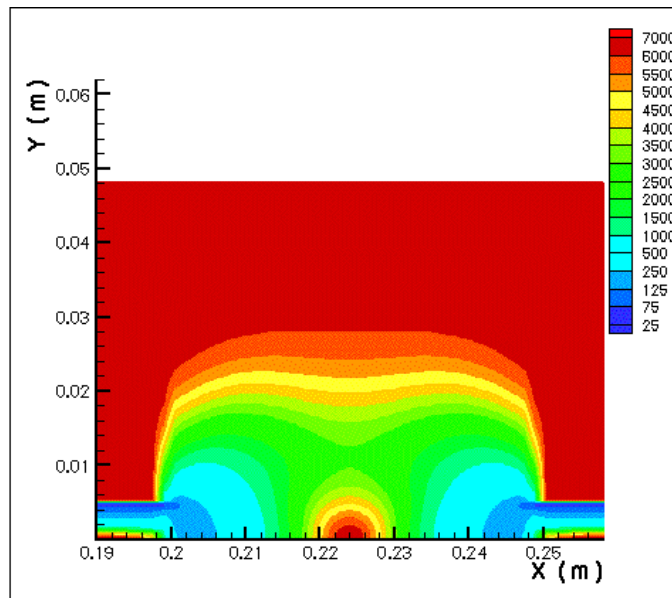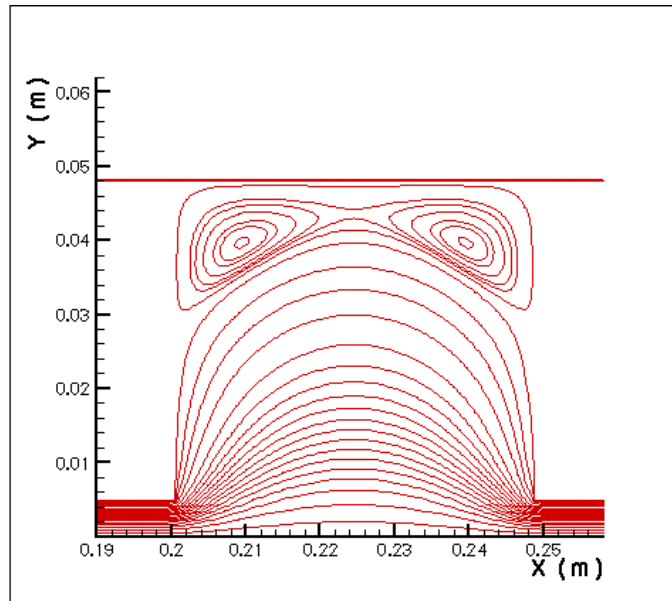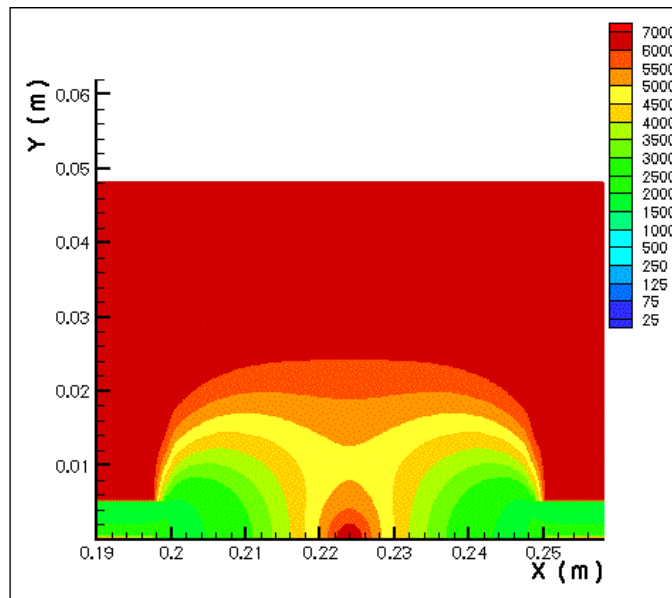

Figure 6: Viscosity function, $\eta_0 = 6.5 \times 10^3$ Pa.s, $\eta_\infty = 0.5$ Pa.s, $\lambda = 0.41$ s^{-1}, $n = 0.25$, and $a = 2$.
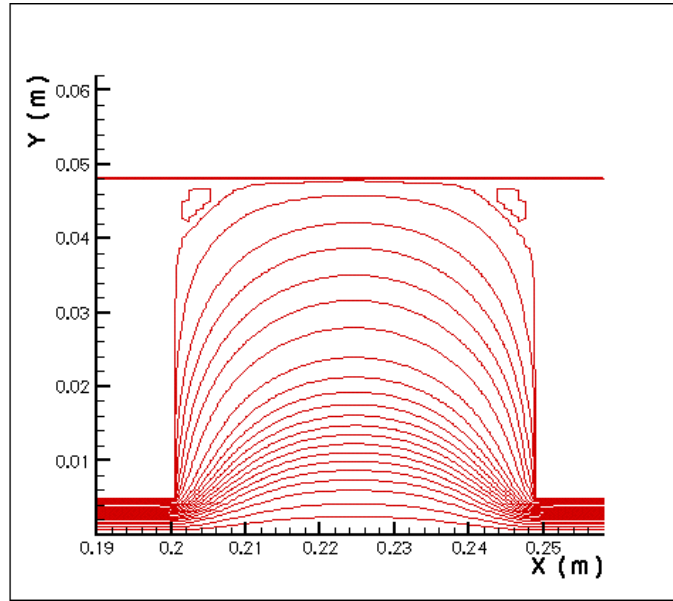
Figure 7: Streamlines, $\eta_0 = 6.5 \times 10^3$ Pa.s, $\eta_\infty = 0.5$ Pa.s, $\lambda = 0.41$ s^{-1}, $n = 0.75$, and $a = 2$.

Figure 8: Viscosity function, $\eta_0 = 6.5 \times 10^3$ Pa.s, $\eta_\infty = 0.5$ Pa.s, $\lambda = 0.41$ s^{-1}, $n = 0.75$, and $a = 2$.

Figure 9: Streamlines, $\eta_0 = 6.5 \times 10^3$ Pa.s, $\eta_\infty = 0.5$ Pa.s, $\lambda = 41$ s^{-1}, $n = 0.5$, and $a = 2$.
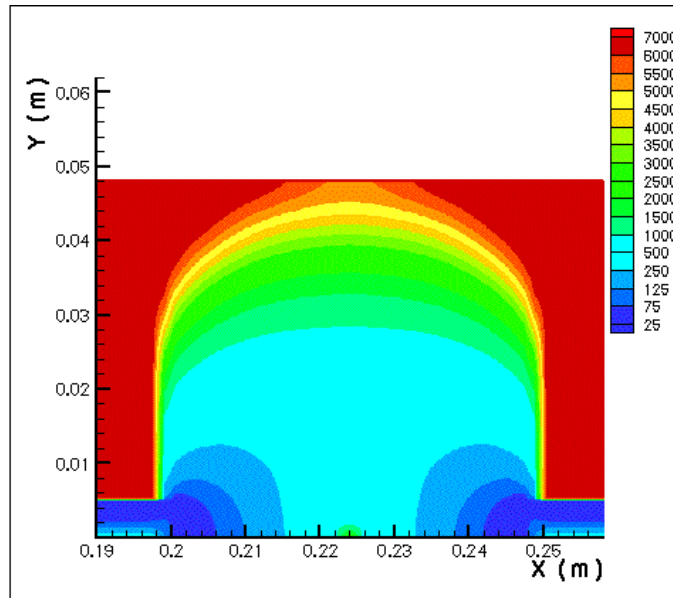

Figure 10: Viscosity function, $\eta_0 = 6.5 \times 10^3$ Pa.s, $\eta_\infty = 0.5$ Pa.s, $\lambda = 41$ s^{-1}, $n = 0.5$, and $a = 2$.
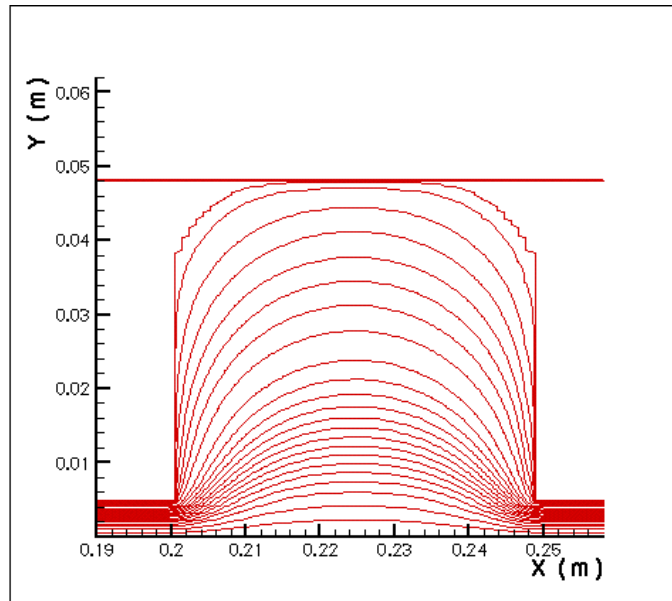
Figure 11: Streamlines, $\eta_0 = 6.5 \times 10^3$ Pa.s, $\eta_\infty = 0.5$ Pa.s, $\lambda = 4100$ s^{-1}, $n = 0.5$, and $a = 2$.
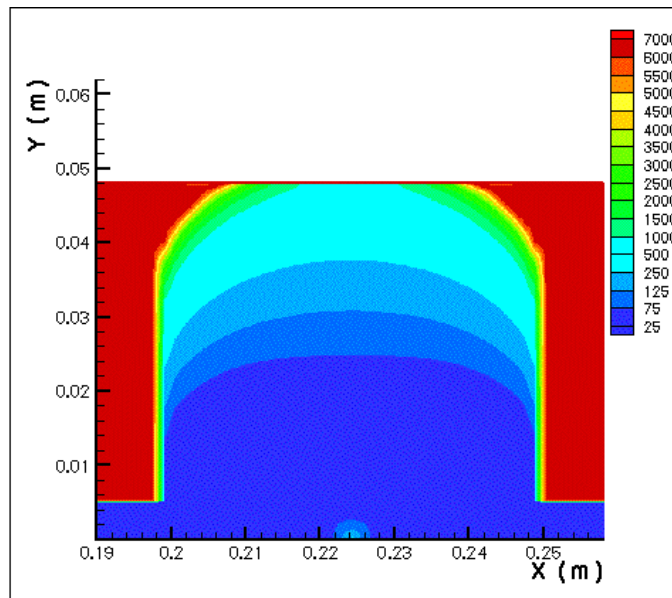

Figure 12: Viscosity function, $\eta_0 = 6.5 \times 10^3$ Pa.s, $\eta_\infty = 0.5$ Pa.s, $\lambda = 4100$ s^{-1}, $n = 0.5$, and $a = 2$.

Figure 13: Streamlines, $\eta_0 = 6.5 \times 10^7$ Pa.s, $\eta_\infty = 0.5$ Pa.s, $\lambda = 0.41$ s^{-1}, $n = 0.5$, and $a = 2$.

Figure 14: Viscosity function, $\eta_0 = 6.5 \times 10^7$ Pa.s, $\eta_\infty = 0.5$ Pa.s, $\lambda = 0.41$ s^{-1}, $n = 0.5$, and $a = 2$.
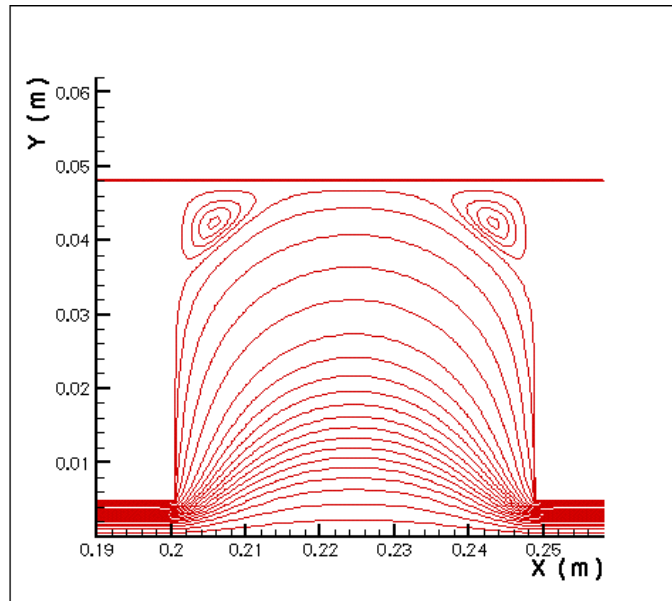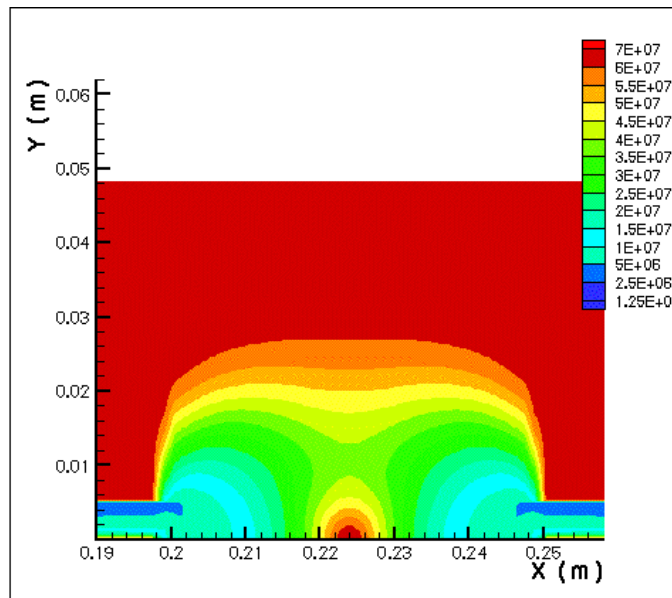
It can be observed that the recirculating zone increases with the power-law exponent n. As n is increased, the viscosity variation is smoother. Therefore, the viscosity at the core region is larger for larger n's. It can be also noted that for small values of n, a plug flow region (a region with the largest value of viscosity, or a region with almost no deformation) appears at the center of core region and at the centerline of the upstream and downstream tubes. This behavior is characteristic of viscoplastic materials, and is expected for viscosity functions with low values of n, where the Carreau model can be viewed as a bi-viscosity model.

Figs. 9–12 show the results obtained for $\lambda = 41$ s^{-1} and 4100 s^{-1}. All other parameters are equal to the ones of the base fluid. It can be observed that as λ is increased, the recirculating zones tends to disappear and the deformation rates increase near the central tube walls, leading to lower levels of viscosity. In these cases, it seems that the material fracture doesn't occur, since the velocities at the core region and near the wall of the central tube are of the same order of magnitude.

Finally, Figs. 13 and 14 show the streamlines and viscosity function for a fluid with a much higher value of η_0 ($\eta_0 = 6.5 \times 10^7$ Pa.s) than the base fluid ($\eta_0 = 6.5 \times 10^3$ Pa.s). The qualitative behaviors are similar to the the ones obtained for the base fluid, as expected, because the only influence of η_0 on the viscosity function is to increase the viscosity levels.

5. Final Remarks

In this paper, a numerical simulation of non-Newtonian flows through an axisymmetric expansion followed by a contraction was performed. The governing equations of mass and momentum were solved via a finite-volume technique. The Generalized Newtonian Fluid constitutive equation and the Carreau viscosity function were used to model the Non-Newtonian fluid behavior.

Numerical results of velocity, viscosity and pressure fields were obtained. The effects of rheological parameters on flow pattern were investigated. It was observed that η_0 has no effect on the flow pattern, and that recirculating zones near the corners increase with the power-law exponent and decrease with the time constant λ. It was also noted a flow transition, as the time constant λ is increased. For lower vaues of λ, a material fracture seems to appear, near the core region of the central tube. This behavior can have strong effects in predicting pressure drop through these flows.

6. Acknowledgment

7. References

Alexandrou, A. N., McGilvreay, T. M. and Burgos, G., 2001, "Steady Herschel-Bulkley fluid flow in three-dimensional expansions", J. Non-Newtonian Fluid Mech., Vol. 100, pp.77–96.

Barnes, H. A., 1999a, "A brief history of the yield stress", Appl. Rheology, Vol. 9, No. 6, pp. 262–266.

Barnes, H. A., 1999b, "Yield stress – a review, or $\pi\alpha\nu\tau\alpha\rho\epsilon$ – everything flows?", J. Non-Newtonian Fluid Mech., Vol. 81, pp. 133–178.

Bird, R.B., Armstrong, R.C. and Hassager, O., 1987, "Dynamics of Polymeric Liquids", Wiley.

Naccache, M.F. and Souza Mendes, P.R., 1997, "Abrupt Expansion Flows of Bingham Materials", Proc. of XIV Brazilian Congress of Mechanical Engineering, in CDROM.

Pak, B., Cho, Y. I. and Choi, S. U. S., 1990, "Separation and Reattachment of Non-Newtonian Fluid Flows in a Sudden Expansion Pipe", J. Non-Newtonian Fluid Mech., Vol. 37, pp.175–199.

Patankar, S. V., 1980, "Numerical Heat Transfer and Fluid Flow", Hemisphere Pub. Corp..

Reis Jr., L. A., "Flow of viscoplastic materials through an abrupt expansion and contraction", Masters Thesis, Department of Mechanical Engineering, Catholic University of Rio de Janeiro, 2003. D Settari, S. and Aziz, K., 1973, "A Generalization of the Additive Correction Methods for the Iterative Solution of Matrix Equations", SIAM J. Num. Anal., Vol. 10, pp.506–521.

Souza Mendes, P. R., Naccache, M. F. and Vinagre, H. T. M., 2000, "On numerical simulations of complex flows of visco plastic materials", Proc. ASME-IMECE, FED-Vol. 252, pp. 17–23.

Vradis, G. C., Ötügen, M. V., 1997, "The Axisymmetric Sudden Expansion Flow of a Non-Newtonian Viscoplastic Fluid", J. of Fluids Engineering, Vol. 110, pp.193–200.